BBA - Molecular Cell Research 1870 (2023) 119384

Contents lists available at ScienceDirect

BBA - Molecular Cell Research

journal homepage: www.elsevier.com/locate/bbamcr

Protective effect of TPP-Niacin on microgravity-induced oxidative stress and mitochondrial dysfunction of retinal epithelial cells

Hong Phuong Nguyen [a,b,1], Seungheon Shin [c,1], Kyung-Ju Shin [a,b,1], Phuong Hoa Tran [a,b], Hyungsun Park [e], Quang De Tran [a,b], Mi-Hyun No [a], Ji Su Sun [d], Ki Woo Kim [d], Hyo-Bum Kwak [b], Seongju Lee [e], Steve K. Cho [c,f,*], Su-Geun Yang [a,b,**]

[a] Inha Institute of Aerospace Medicine, Inha University College of Medicine, Incheon 22332, Republic of Korea
[b] Department of Biomedical Science, BK21 FOUR program in Biomedical Science and Engineering, Inha University College of Medicine, Incheon 22332, Republic of Korea
[c] Department of Biomedical Science and Engineering, Gwangju Institute of Science and Technology (GIST), Gwangju 61005, Republic of Korea
[d] Departments of Oral Biology and Applied Biological Science, BK21 FOUR, Yonsei University College of Dentistry, Seoul 03722, Republic of Korea
[e] Department of Anatomy, College of Medicine, BK21 FOUR Program in Biomedical Science & Engineering, Inha University, Incheon 22212, Republic of Korea
[f] School of Life Sciences, Gwangju Institute of Science and Technology (GIST), Gwangju 61005, Republic of Korea

ARTICLE INFO

Keywords:
Microgravity (μG)
ROS
ARPE19 cells
Autophagy
Mitophagy
TPP-Niacin

ABSTRACT

Adverse effects of spaceflight on the human body are attributed to microgravity and space radiation. One of the most sensitive organs affected by them is the eye, particularly the retina. The conditions that astronauts suffer, such as visual acuity, is collectively called a spaceflight-associated neuro-ocular syndrome (SANS); however, the underlying molecular mechanism of the microgravity-induced ocular pathogenesis is not clearly understood. The current study explored how microgravity affects the retina function in ARPE19 cells *in vitro* under time-averaged simulated microgravity (μG) generated by clinostat. We found multicellular spheroid (MCS) formation and a significantly decreased cell migration potency under μG conditions compared to 1G in ARPE19 cells. We also observed that μG increases intracellular reactive oxygen species (ROS) and causes mitochondrial dysfunction in ARPE19 cells. Subsequently, we showed that μG activates autophagic pathways and ciliogenesis. Furthermore, we demonstrated that mitophagy activation is triggered *via* the mTOR-ULK1-BNIP3 signaling axis. Finally, we validated the effectiveness of TPP-Niacin in mitigating μG-induced oxidative stress and mitochondrial dysfunction *in vitro*, which provides the first experimental evidence for TPP-Niacin as a potential therapeutic agent to ameliorate the cellular phenotypes caused by μG in ARPE19 cells. Further investigations are, however, required to determine its physiological functions and biological efficacies in primary human retinal cells, *in vivo* models, and target identification.

1. Introduction

The effects of microgravity and space radiation after space travel on the human body have been well documented since the first human spaceflight in 1961 [1]. The primary symptoms that the astronauts have described immediately after space shuttle or International Space Station (ISS) missions include bone and muscle mass reduction, cardio-vascular imbalances, circadian misalignment, and various vestibular and sensory imbalances [2]. In particular, the eye is severely sensitive to cephalad fluid shift caused by microgravity which induces several neuro-ophthalmic alterations, such as optic disc edema, globe flattening, choroidal and retinal folds, hyperopic refractive error shifts, nerve fiber

Abbreviations: MCS, Multicellular spheroids; ROS, Reactive oxygen species; RPE, Retinal pigment epithelium; TPP, Triphenylphosphonium; SANS, spaceflight-associated neuro-ocular syndrome.

* Correspondence to: S. K. Cho, Department of Biomedical Science and Engineering, School of Life Sciences, Gwangju Institute of Science and Technology (GIST), Gwangju 61005, Republic of Korea.

** Correspondence to: S.-G. Yang, Department of Biomedical Science, Inha University College of Medicine, 366 Seohae-daero, Jung-gu, Incheon 22332, Republic of Korea.

E-mail addresses: scho@gist.ac.kr (S.K. Cho), Sugeun.Yang@inha.ac.kr (S.-G. Yang).

[1] These authors contributed equally: H. P. Nguyen, S. Shin, and K.J. Shin

https://doi.org/10.1016/j.bbamcr.2022.119384
Received 23 June 2022; Received in revised form 11 October 2022; Accepted 17 October 2022
Available online 24 October 2022

layer infarcts, and visual acuity reduction, collectively termed spaceflight associated neuro-ocular syndrome (SANS) [3]. In addition, the spaceflight environment induces oxidative stress that results in apoptosis in mouse retina [4]. Oxidative stress is an imbalance between the production levels of reactive oxygen species (ROS) and detoxification of its harmful effects through neutralization by antioxidants. ROS can be derived from the mitochondrial respiratory chain when the electrons are transported from complexes I and III or from the increased formation of $O_2^{\bullet}$ radicals by an incomplete reaction during a one-electron oxygen reduction under hypoxic conditions [4–8]. Superoxide dismutase converts superoxides, which are membrane-impermeable radicals, into membrane-permeable H_2O_2. Then, mitochondria-generated H_2O_2 is further reduced to produce hydroxyl radical $^{\bullet}OH$, which is highly toxic and quickly reacts with several metabolites resulting in oxidative stress in cells [9].

Retinal pigment epithelial (RPE) cells are a cuboidal monolayer of non-neuronal epithelial cells located between photoreceptors and choroidal capillaries in the neurosensory part of the retina to facilitate substance exchange [6,7]. Since RPE provides the structural basement of the retina and holds various functions for nutritional exchange and maintaining visual cycles, the malfunction of RPE affects the overall optical system [25]. Also, oxidative stress from multiple sources damages RPE cells, leading to ocular pathogenesis, including reduced visual acuity. Because of the high oxygen consumption of retinal cells and the phagocytic nature of RPE cells, oxidative stress is more prominent in RPE cells [6]. Furthermore, mitochondrial DNA (mtDNA), which lacks histone proteins, becomes more susceptible to oxidative stress caused by ROS than nuclear DNA [1]. Typically, oxidative stress is minimized by antioxidants and a range of efficient repair systems. We performed our study using ARPE19 cells, which is a spontaneously arising human RPE cell line with a normal karyotype [2,6].

Oxidative stress can lead to non-specific post-translational protein modification and protein aggregation, which is linked to mitochondrial dysfunction [2,6,7]. Autophagy is an essential pathological response in cross-talk with ROS and redox signaling pathways [8,10,11]. Autophagy activation is often mediated by AMPK through mTOR, which closely regulates the process *via* phosphorylation-dependent ULK1 [11–13]. As a part of the autophagy pre-initiation complex, ULK1 activates the downstream autophagy initiation complex by triggering a cascade of proteins such as Beclin-1 [5,12].

To specifically minimize mitochondria-generated ROS, we modified a newly synthesized TPP-niacin conjugate. The selective targeting of antioxidants by covalent conjugation with lipophilic triphenylphosphonium (TPP) cation towards mitochondria to reduce the oxidative stress caused by mitochondrial dysfunction is well documented as an effective strategy [14–17]. In a recent investigation, TPP-Niacin was evaluated as an effective therapeutic agent to reduce oxidative stress in age-related macular degeneration [7].

However, the underlying mechanism of how microgravity-induced oxidative stress degrades visual acuity by affecting the retinal function has not been clearly delineated. In this study, we investigate how ARPE19 cells are affected *in vitro* by time-averaged simulated microgravity (μG) generated by clinostat [18,19], which induces the formation of multicellular spheroids (MCS), decreases cell migration potency, and elevates intracellular ROS as well as mitochondria dysfunction. Subsequently, we showed that μG activates autophagic pathways and ciliogenesis. Furthermore, we demonstrated that mitophagy activation was triggered *via* the mTOR-ULK1-BNIP3 signaling axis. Finally, we validated the effectiveness of TPP-Niacin in mitigating μG-induced oxidative stress and mitochondrial dysfunction *in vitro* in ARPE19 cells.

2. Materials and methods

2.1. Simulated microgravity (μG)

To establish the microgravity environment of *in vitro* culture, the gravity controller, Gravite® (Space Bio-Laboratories Co., Ltd), was used. This device produces a similar climate to outer space (10^{-3}G) by rotating a sample around two axes, integrating the gravity vector with the temporal axis [18]. Eventually, the summation of the gravity vector in a spherical space results in simulated microgravity at the center of the device.

2.2. Cell culture

ARPE19 (human adult retinal pigment epithelium cell line from ATCC) cells were seeded at 5000 cells/ T25 flask and cultured in DMEM/F12 (11320033, Gibco™) medium supplemented with 10 % (*v*/v) heat-inactivated fetal bovine serum (SH30071.03, HyClone), 100 μg/ml of streptomycin, and 100 U/ml of penicillin (15140122, Gibco™). The cells were cultured at 37 °C in a humidified 5 % CO2 atmosphere, and the medium was changed every three days for cell maintenace and experiments.

2.3. Cell viability

Cell viability was measured using the CELLOMAXTM Viability Assay kit (Precaregene Co., Seoul, Korea). UV absorption at 450 nm wavelength was measured using an Infinite M200 microplate reader (Tecan, Zürich, Switzerland). The percent of cell viability was calculated using Prism v5.0 (GraphPad Software Inc., La Jolla, CA).

Fluorescent microscopic images of proliferating (blue) and dead cells (green) was determined using the ReadyProbes™ Cell Viability Imaging Kit (R37609, Invitrogen™). ARPE19 cells were seeded at 10^4 cells on the cell culture slide hybrid well (333,031, SPL). Briefly, two drops of NucBlue® Live reagent and NucGreen® Dead reagent were added per ml of culture media, respectively, and samples were incubated for 15 min at 37 °C in a humidified atmosphere containing 5 % CO_2. Finally, cells were mounted with ProLong Gold Antifade Mountant (P36930, Invitrogen™), and images were acquired using a 20× objective by a fluorescent microscope IX81 (Olympus Optical).

2.4. ROS detection assay

The intracellular levels of ROS were measured using the 2′,7′-Dichlorofluorescin diacetate molecular probes (D6883, Sigma-Aldrich). Cells were incubated with 10 μM DCFH-DA diluted with the low FBS culture media (1 % FBS) for 30 min at 37 °C, then washed and resuspended in PBS at 1 × 10^6 cells/ml. The cells were analyzed using BD Accuri™ C6 Plus Flow Cytometer (BD bioscience) at excitation and emission wavelengths of 488 and 525 nm. Untreated cells were used as a control. The results were expressed as fluorescence intensity of dichlorofluorescein (DCF) compared to the control. The results were analyzed using Image J (National Institutes of Health).

2.5. Mitochondrial mass analysis

ARPE19 cells were seeded at 10^4 cells on a cell culture slide hybrid well (333,031, SPL). Cells were incubated with MitoTracker Green FM (M7514, Invitrogen™) at 100 nM for 15 min. Finally, cells were mounted with ProLong Gold Antifade Mountant (P36930, Invitrogen™), and images were acquired using a 20× objective by a fluorescent microscope IX81 (Olympus Optical). The results were analyzed using Image J.

2.6. Reverse transcription (RT)-PCR and quantitative real-time RT-PCR (qRT-PCR)

Gene expression analysis was performed by quantitative real-time RT-PCR using 18S ribosomal RNA (rRNA) to normalize target gene expression for each sample. Primers and probes were designed by Primer Express (Applied Biosystems) following the manufacturer's guidelines.

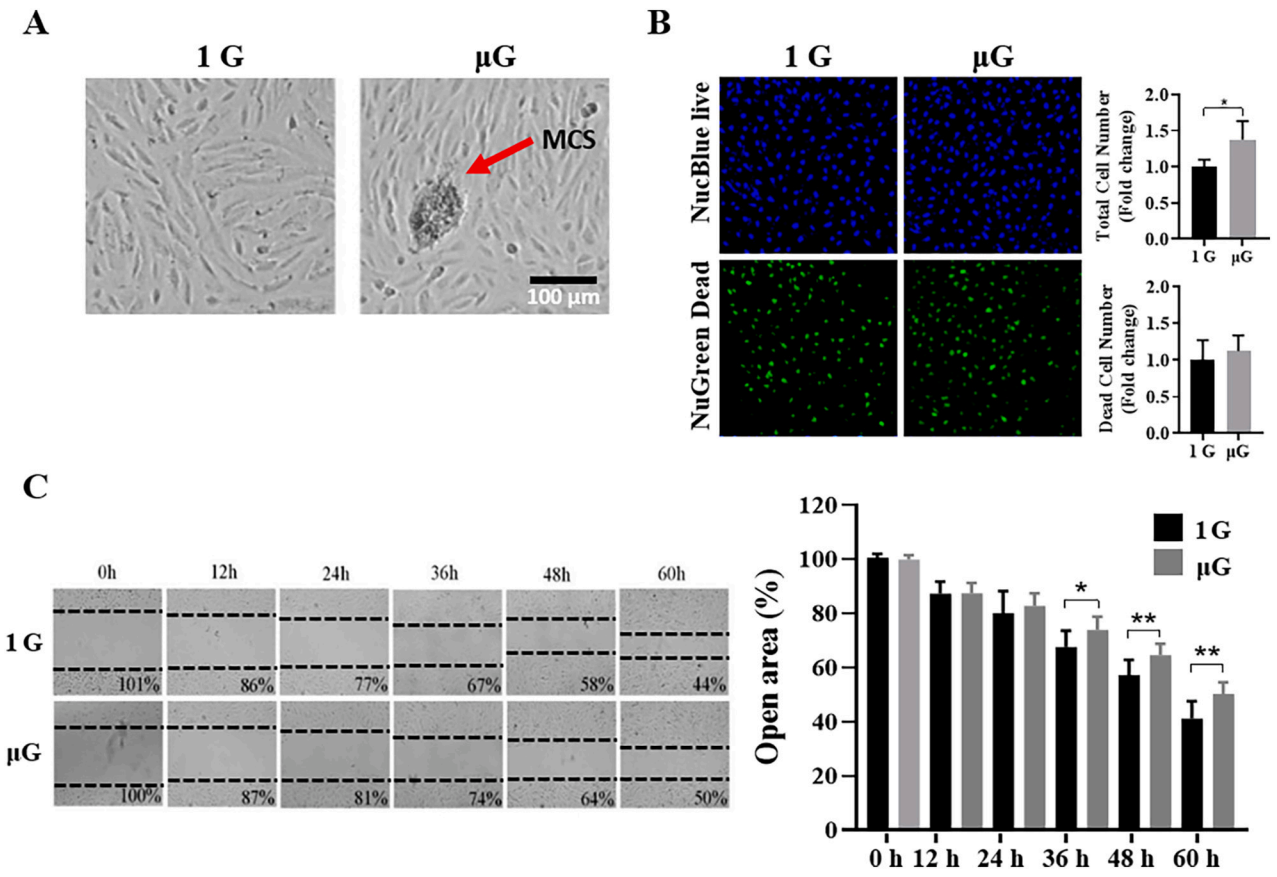

Fig. 1. μG induces MCS and decreases cell migration potency in ARPE19 cells.
(A) Cell morphological changes in ARPE19 cells under μG. Phase-contrast microscopy images of 1G control (left) and ARPE19 cells after a three-day μG exposure (right). The red arrow indicates the multicellular spheroid (MCS) formation. Scale bar: 100 μm. (B) Changes in ARPE19 cell proliferation and apoptosis after a three-day μG exposure. Fluorescent microscopic images of proliferating (blue) and dead cells (green) were analyzed under μG and compared to 1G conditions. *Significant ($P < 0.05$). (C) Cell migration potential changes in ARPE19 cells after a three-day μG exposure. Phase-contrast microscopy images of 1G control (top) and ARPE19 cells under μG (bottom) conditions for gap closure. Scale bars:100 μm. Error bars represent the standard deviation.

PCR reactions were performed in a 20 μl final volume adding 1 μl cDNA from each sample, using TaqMan Universal PCR mix (4,304,437, Applied Biosystems). For PCR reaction, ABI TaqMan Gene Expression Assays (Applied Biosystems) were used to detect ATP5F1A. PCR amplification was performed on 384-well plates using the default cycling conditions, and fluorescence was detected by the ABI 7900HT Sequence Detection System (Applied Biosystems).

2.7. Western blot analysis

Proteins were extracted with RIPA Lysis and Extraction Buffer (89,900, Thermo Scientific™). Equal amounts of protein were separated by 12 % sodium dodecyl sulfate-polyacrylamide gel electrophoresis (SDS-PAGE) and wet-blotted on polyvinylidene difluoride (PVDF, 1620177, Bio-rad) membranes. The membranes were blocked with 5 % non-fat milk (232,100, BD biosciences) in Tris-buffered saline plus 1 % Tween-20 and probed with primary antibodies (anti-SQSTM1/p62; 39749S, anti-ATG5; 12,994 T, anti-Beclin-1; 3495 T, anti-LC3A/B; 12,741 T, anti-ATG12; 4180 T, anti-p-AMPK; 2531S, anti-AMPK; 2532S, anti-p-mTOR; 2971S, anti-mTOR; 2972S, anti-p-ULK; 6888 T, anti-ULK; 5869 T, anti-GAPDH; 2118S, Cell Signaling Technology, MA, and anti-BNIP3; MBS1499353, MyBioSource,CA, anti-cyclophilin D; PA3–022, Invitrogen MA. Protein bands were stained using HRP-conjugated secondary antibodies (mouse anti-rabbit IgG-HRP; sc-2357, Santa Cruz Biotechnology, TX). Images were developed using the enhanced chemiluminescence system (Western Lightning Plus-ECL, PerkinElmer, MA) and visualized with a luminescent image analyzer (LAS-4000, Fujifilm, Janpan). Quantitative densitometry of the immunoreactive bands was performed using ImageQuant TL software (GE Healthcare, IL) or Image J. (NIH, USA).

2.8. Cilia staining

For *in vitro* immunofluorescence for cilia, ARPE19 cells were washed with 1× phosphate-buffered saline (PBS, pH 7.4) (AM9624, Invitrogen™) and fixed with 4 % (*w/v*) paraformaldehyde (PFA) (P6148, Sigma-Aldrich, MO), dissolved in PBS for 10 min at room temperature (RT). Cells were washed in PBS 3 times for 10 min each and permeated in 0.1 % Triton X-100 (X100, Sigma-Aldrich, MO) in PBS (*v*/v) for 20 min. Subsequently, cells were blocked with 1 % bovine serum albumin (BSA) (BSAS-AU, Bovogen, Australia) prepared in PBS containing 0.1 % Triton X-100 (PBT) and incubated overnight at 4 °C with primary antibodies against acetylated α-tubulin (T7451, Merck) in 1 % BSA-PBT. After a day, 3 times washing in PBS, cells were incubated with Alexa Fluor 488 conjugated antibodies (A28175, Invitrogen, MA) at room temperature (RT) for 1 h. After washing, the cells were mounted on glass slides and were visualized by a confocal laser microscope.

2.9. Chemical synthesis

TPP-Niacin was chemically synthesized as reported previously [7]. Briefly, 1.2 ml of Tetrabutylammonium fluoride (1.0 M in THF, 1,2 mmol, 1.2 eq, 216,143, Sigma-Aldrich, MO) was added at room temperature to a solution of Nicotinic acid (123.11 mg, 1.0 mmol, 1.0 eq) in

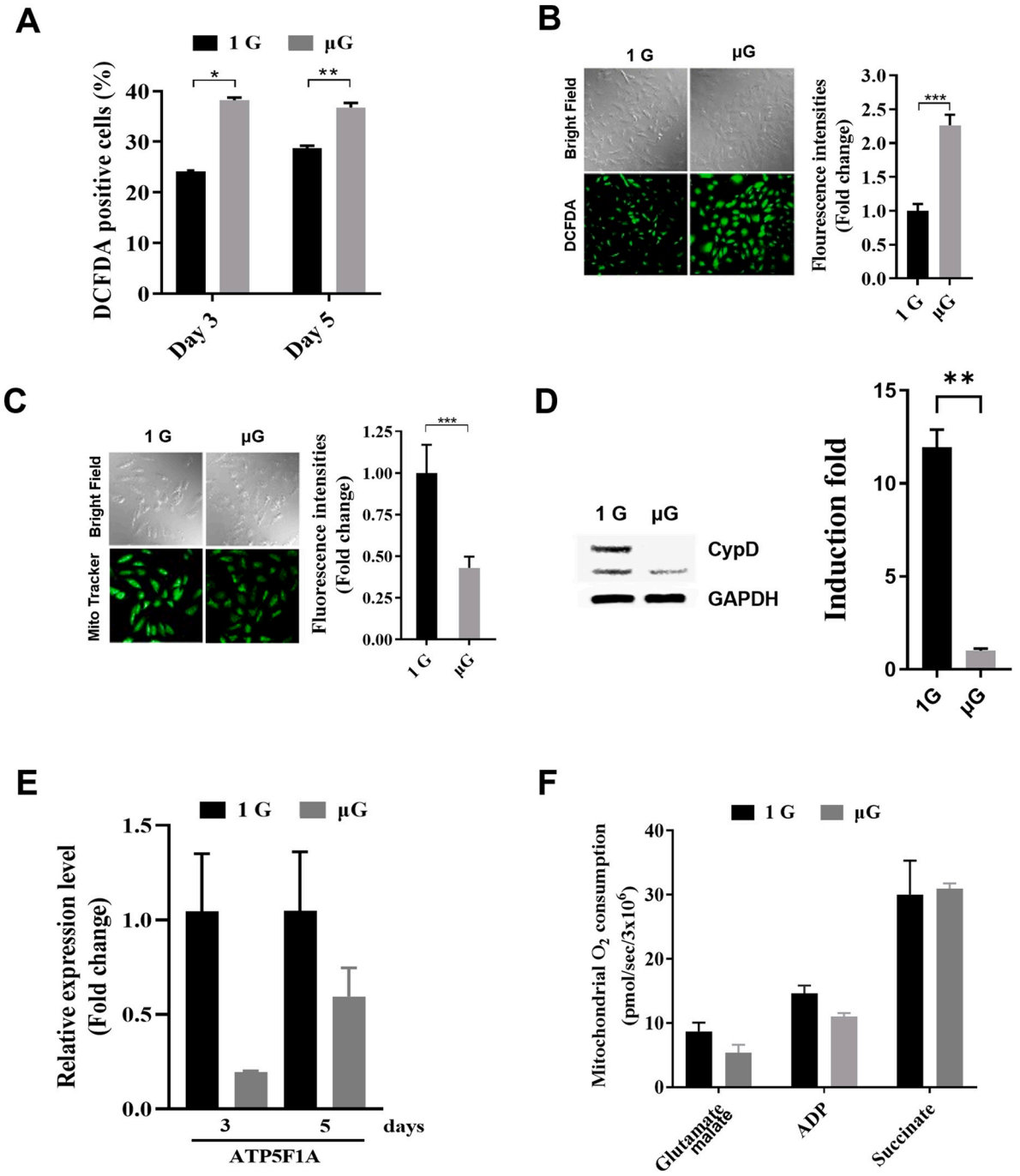

Fig. 2. Elevated intracellular ROS and mitochondria dysfunction in ARPE19 cells by μG
(A) ARPE19 cells incubated in 1G or μG conditions for 3 days or 5 days were harvested. ROS generation was determined by 2′,7′-dichlorofluorescein diacetate (DCFDA) staining. (B—C) Phase-contrast (top) and fluorescence (bottom) microscopic images of 1G control and ARPE19 cells after a three-day μG exposure stained with DCFDA (B) or MitoTracker™ Green (C). The fold-change of fluorescent intensity was normalized to the 1G condition. (D) Cyclophilin D (CypD) immunoblot analysis of ARPE19 cells after a 5-day μG exposure. GAPDH is used as a loading control. (E) qRT-PCR analysis of ATP synthase (ATP5F1A) mRNA level in ARPE19 cells after a three-day μG exposure. (F) Mitochondrial OCR (O_2 consumption rate) analysis in ARPE19 cells after a three-day μG exposure (black bar) *vs* 1G condition (white bar). Glutamate/malate were used to study complex I-mediated respiration. Succinate was used to analyse complex II mediated respiration. ADP was used to investigate respiration activity in the presence of ADP. Each bar represents the mean ± SD of three independent experiments. *Significant ($P < 0.05$).

DMF (5.0 ml), and the mixture was stirred for 20 min. Then, the solution was allowed to react with 621.48 mg of (4-Bromobutyl) triphenylphosphonium bromide (1.3 mmol, 1.3 eq, 272,132, Sigma-Aldrich, MO) for 60 min at the same temperature, and progress of the reaction was monitored by TLC. Then, DMF was removed by high vacuum; the resulting crude product was purified by flash chromatography (EtOAc: MeOH, 3:1) to obtain the TPP-Niacin product. All chemicals for TPP-Niacin synthesis were purchased from Sigma-Aldrich (MO, USA) and used without further purification.

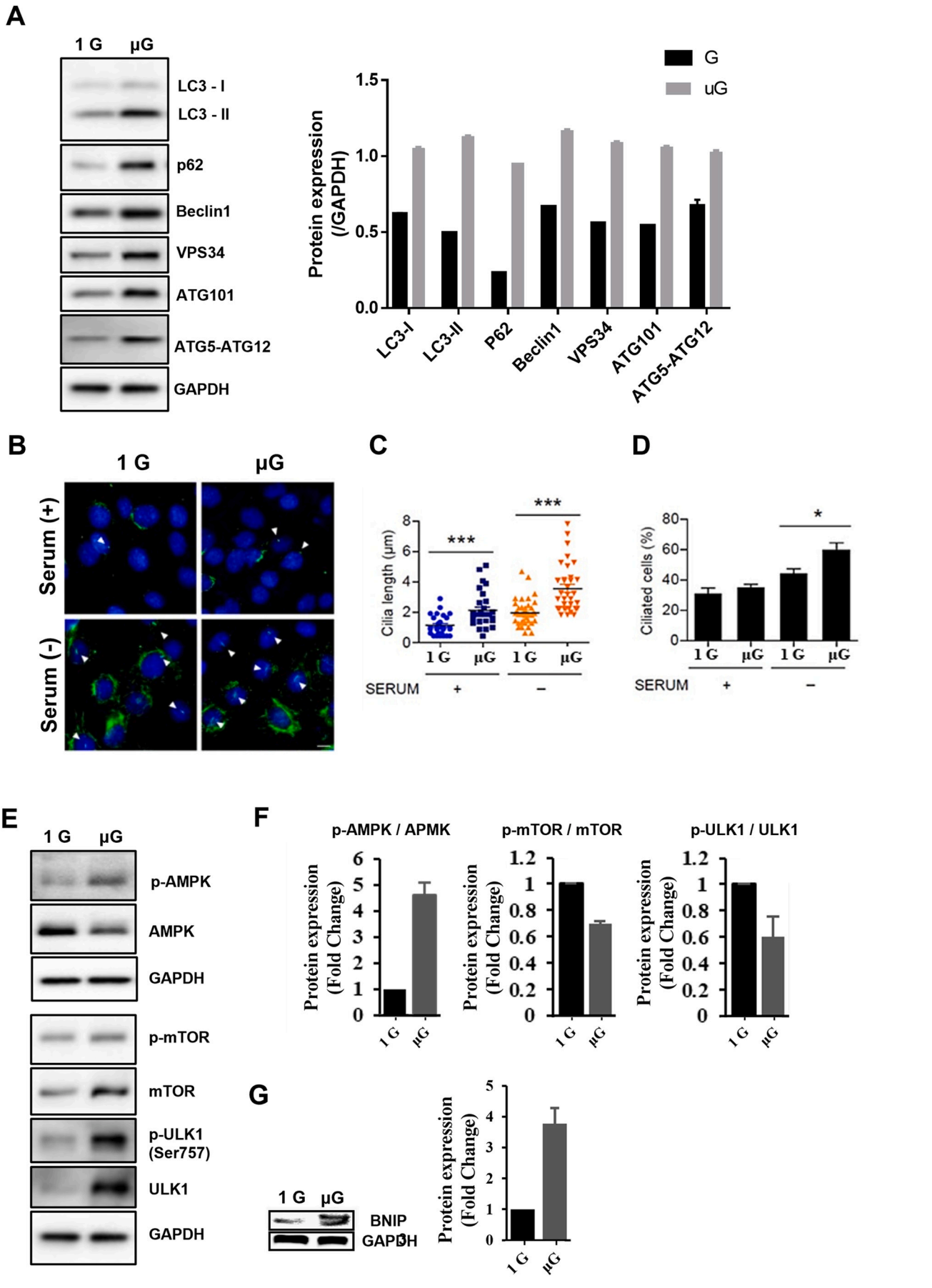

(caption on next page)

Fig. 3. μG activates the autophagic pathways and induces ciliogenesis in ARPE19 cells.
(A) Immunoblot analysis of autophagy-related proteins (LC3, P62, Beclin1, VPS34, ATG101, ATG5-ATG12) in ARPE19 cells after a three-day μG exposure. GAPDH is used as a loading control. (B—D) Qualitative (B) and quantitative (C and D) measurement of ciliogenesis in ARPE19 cells after a three-day μG exposure. Acetylated tubulin (green) and nuclei (blue) were visualized by immunofluorescence microscopy with or without serum starvation for 24 h (B). Cilia length (C) and ciliated cell number (D) were quantified in ARPE19 cells after a three- day μG exposure with or without serum starvation for 24 h. (*E*-G) μG induces mitophagy *via* AMPK-mTOR-ULK1-BNIP3 signaling pathways. Representative immunoblot showing phosphorylation and total levels of AMPK, mTOR, and ULK1 in ARPE19 cells after a three-day μG exposure (E). Quantitative ratios of pAMPK/AMPK, p-mTOR/mTOR, and p-ULK1(Ser757)/ULK1 (F). Densitometric analyses of pAMPK/AMPK, p-mTOR/mTOR, and p-ULK1(Ser757)/ULK1 ratios were determined after normalization to GAPDH, respectively. BNIP3 immunoblot (right) of ARPE19 cells after a three-day μG exposure and the fold change of BNIP3 under μG was determined after normalization to GAPDH (G). Each bar represents the mean ± SD of three independent experiments. $*p < 0.05$, and $***p < 0.001$.

2.10. Mitochondrial O_2 respiration

Mitochondrial O_2 consumption rate was measured by ultilizing a high-resolution respirometry instrument (Oroboros Oxygraph-2 k, Innsbruck). The experimemt was conducted at 30 °C in air-saturated by using buffer Z under the following protocols: 5 mM glutamate, complex I substrate (G5889, Sigma-Aldrich) + 2 mM malate, complex I substrate, state 2 conditions (M7397, Sigma-Aldrich) followed by sequential additions of 4 mM ADP (state 3 conditions) and 10 mM succinate,complex II substrate (S2378, Sigma-Aldrich). Glutamate/malate were used to study complex I-mediated respiration and succinate was used to analyse complex II mediated respiration. ADP was used to investigate respiration activity in the presence of ADP.

2.11. Cell migration assay

ARPE19 cells (1×10^4) were seeded in DMEM/F12 supplemented with 10 % FBS in T25 flasks with the SPL Scar block (SPL Life Sciences, Korea) to create a defined area across. The cells were incubated for 6 h at 37 °C in a humidified 5 % CO2, allowing cells to adhere on the surface. Then, the SPL Scar block was removed, and cells were kept at microgravity or normal environment. The cell migration was observed under the microscope at different time points from 12 to 60 h. The open area was calculated by ImageJ. Percentage of open areas was determined between each indicated time point with 0 h relatively.

2.12. Graphs and statistical analysis

Graphs and statistics: Prism v5.0 (GraphPad Software Inc.) software was used to prepare graphs. Results were expressed as mean ± standard error (SE). A *p*-value <0.05 was considered significant.

3. Results

3.1. μG induces MCS and decreases cell migration potency in ARPE19 cells

In an animal study, the spaceflight environment has been shown to affect global gene expressions, including the significant alterations in visual pathways [4]. To better understand the underlying mechanism of how microgravity (μG) causes physiological changes in astronauts' vision after space travel, we observed morphological changes in ARPE19 cells, which is a human retina pigment epithelial cell line, under time-averaged simulated microgravity (μG) conditions *in vitro* that was generated by clinostat as described in the previous studies [11,19,20]. We found multicellular spheroids (MCS) in ARPE19 cells under μG conditions compared to 1G (Fig. 1A), which agreed with previous reports [20,21]. We also found that cell proliferation increased under μG compared to 1G with no discernible changes in the number of dead cells (Fig. 1B). Recently, it has been reported that microgravity may cause the inhibitory effect of cell migration on human cells [24]. To elucidate the effect of microgravity on cell migration of ARPE19, we cultured the cells in the clinostat and measured its migration capacity at the indicated times from 0 to 36 h. The result showed that μG began to inhibit the migration from 24 h and significantly decreased the cell migration under μG compared to 1G from 36 to 60 h (Fig. 1C).

3.2. Elevated intracellular ROS and mitochondria dysfunction in ARPE19 cells by μG

The spaceflight environment is known to cause ocular tissue abnormality by oxidative stresses [3,4,22]; we, therefore, assessed whether the μG induces oxidative stress in ARPE19 cells *in vitro*. The ROS production in the cells under μG significantly increased compared to normal gravity, as indicated by a significant increase in DCFDA positive cells (Fig. 2A and B). We then measured the change in mitochondrial biogenesis and found that the μG led to a marked reduction in mitochondrial mass (>50 %) under μG conditions compared to normal gravity (Fig. 2C). Simultaneously, μG also reduced the protein expression of cyclophilin D (CypD) and mRNA expression levels of the mitochondrial ATP synthase gene (ATP5F1A) while decreasing mitochondrial oxygen consumption in ARPE19 cells (Fig. 2D and F). Together, these data implicate μG for the elevated intracellular ROS and the mitochondrial dysfunction in ARPE19 cells.

3.3. μG activates the autophagic pathways and induces ciliogenesis in ARPE19 cells

Autophagic pathways may also be induced as a pathogenic response to μG conditions in ARPE19 cells due to inadequate ROS levels and dysfunctional mitochondria. To validate that the autophagy activation was induced by μG, protein expression levels of autophagy-related genes (LC3, p62, Beclin1, VPS34, Atg101, and Atg5-Atg12) were analyzed by Western blot analysis (Fig. 3A). The results revealed that every autophagy-related gene tested was significantly upregulated, confirming the activation of autophagy pathways in ARPE19 cells under *in vitro* simulated microgravity condition.

Next, we investigated the effect of μG on cellular ciliogenesis, which is closely linked to autophagy activation. Qualitative and quantitative confocal microscopy analyses revealed that both ciliated cell numbers and the cilia length were significantly increased under μG compared to 1G in ARPE19 cells grown in serum-free media, demonstrating the activation of autophagy during nutrient deprivation (Fig. 3B and D). Interestingly, μG also induced nutrient-independent cilia length increase in ARPE19 cells, suggesting that μG may affect ARPE19 cell ciliogenesis through multiple mechanisms (Fig. 3C).

3.4. μG induces mitophagy via AMPK-mTOR-ULK1-BNIP3 signaling pathways

We next explored the mechanism of autophagy induced by μG. AMPK is one of the main stress-sensing enzymes that activate autophagy by suppressing mTOR phosphorylation [11,12]. Thus, we analyzed the ratios of p-AMPK/AMPK and p-mTOR/mTOR under μG compared to normal gravity. Fig. 3E and F show that μG increased AMPK phosphorylation in ARPE19 cells, which was accompanied by decreasing mTOR phosphorylation. Decreased mTOR phosphorylation subsequently reduced the phosphorylation of ULK1 at serine 757 position which inhibits the activation of ULK1 [23]. Interestingly, we noticed that μG also affects the total protein levels of AMPK, mTOR, and ULK1.

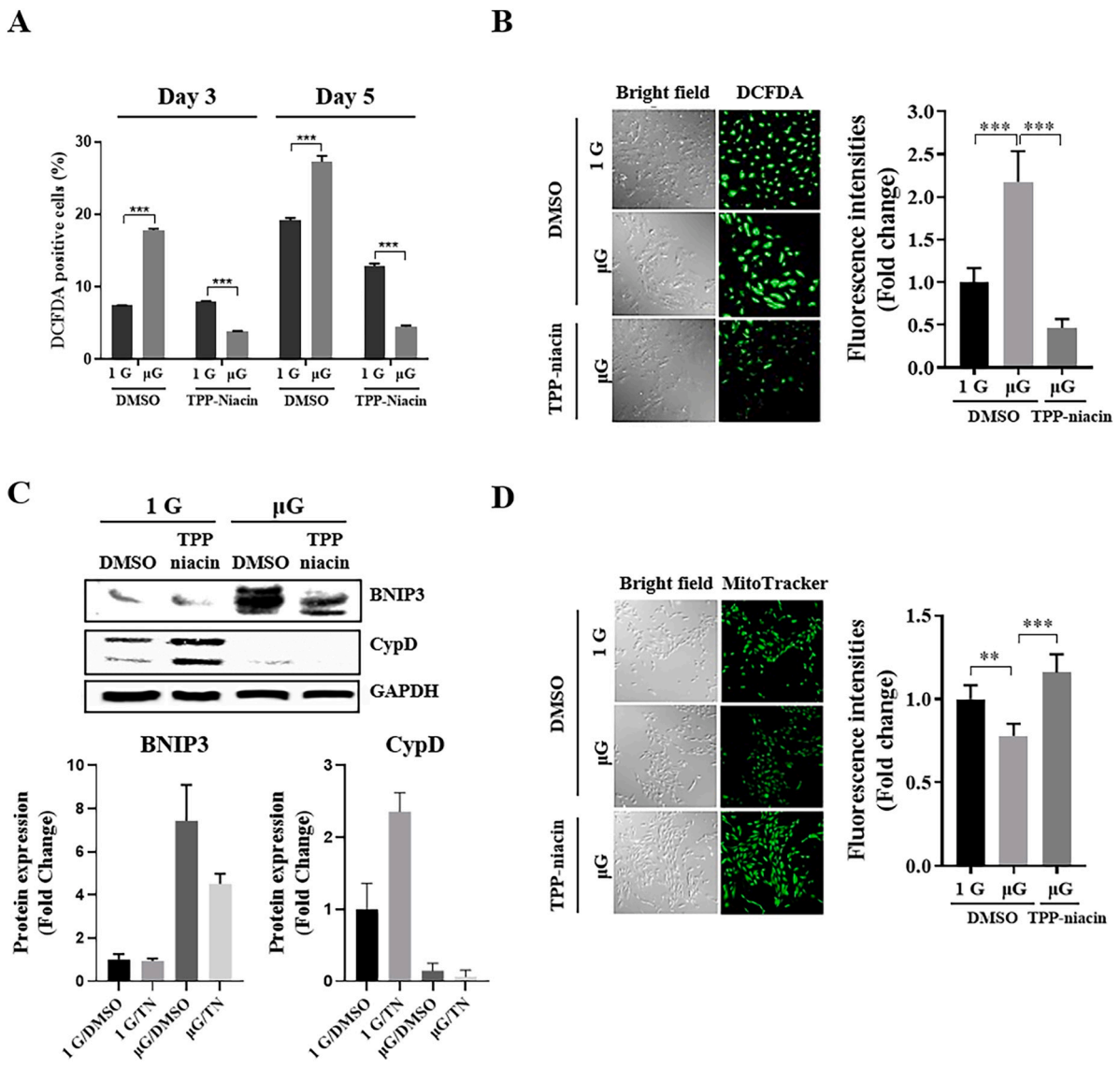

Fig. 4. TPP-Niacin treatment mitigates μG -induced oxidative stress and mitochondrial dysfunction in ARPE19.
(A-D) ARPE19 cells incubated in 1G or μG conditions for either 3 days or 5 days were harvested. ROS generation was determined by 2′,7′-dichlorofluorescein diacetate (DCFDA) staining. The cells were treated with either DMSO or TPP-Niacin (50 μM) for 2 h. While intracellular ROS level was monitored by DCFDA staining, the protective effects of TPP-Niacin against μG-induced ROS generation in ARPE19 cells were assessed by reduction in DCFDA positive cells and fluorescence intensity with the treatment (A and B). The fold-change of fluorescent intensity was normalized to 1 G control. Mitophagy activation marker BNIP3 (C) and phase-contrast (left) and MitoTrackerGreen (right) monitoring for mitochondria biogenesis (D) were shown to demonstrate the protective effects of TPP-Niacin against μG-induced mitochondrial dysfunction. GAPDH was used as a loading control. The fold-change of fluorescent intensity was normalized to 1G control. *$p < 0.05$, **$p < 0.01$, ***$p < 0.001$ *versus* the gravity group were considered statistically significant differences.

Next, we assessed BNIP3 protein stability because BNIP3 proteasomal degradation is inhibited by ULK1, which promotes BNIP3-dependent mitophagy [12,13,23], revealing that the BNIP3 protein level increased by 3.8-fold under μG compared to 1G (Fig. 3G).

Together, these data imply that the AMPK-mTOR pathway is a vital regulator involved in μG-induced autophagic responses in ARPE19 cells, and ULK1 modulates BNIP3-dependent mitophagy activation.

3.5. TPP-Niacin treatment mitigates μG-induced oxidative stress and mitochondrial dysfunction in ARPE19

Because we have previously shown that TPP-Niacin mitigated oxidative stress in the retina *in vitro* [7], we have tested the efficacy of TPP-Niacin in ARPE19 cells grown under μG. Flow cytometry analyses revealed that DCFDA positive cell numbers were significantly reduced by TPP-Niacin treatment (50 μM) under μG (Fig. 4A). Confocal microscopy analysis also showed that TPP-Niacin reverted the elevated ROS production in ARPE19 cells caused by μG (Fig. 4B). Furthermore, TPP-Niacin reduced BNIP3 protein stability that is associated with mitophagy activation but failed to rescue the CypD expression back to normal (Fig. 4C). Confocal microscopy showed a similar reversion of mitochondrial function and biogenesis monitored by MitoTracker Green after TPP-Niacin treatment under μG conditions (Fig. 4D). Taken together, these data validate the protective effect of TPP-Niacin against μG-induced oxidative stress and mitochondrial dysfunction in ARPE19 cells.

4. Discussion

A common adverse effect reported by astronauts after returning to earth from space is decreased visual acuity [3,8,9]. A mouse model study has revealed that retinal performance was significantly affected due to

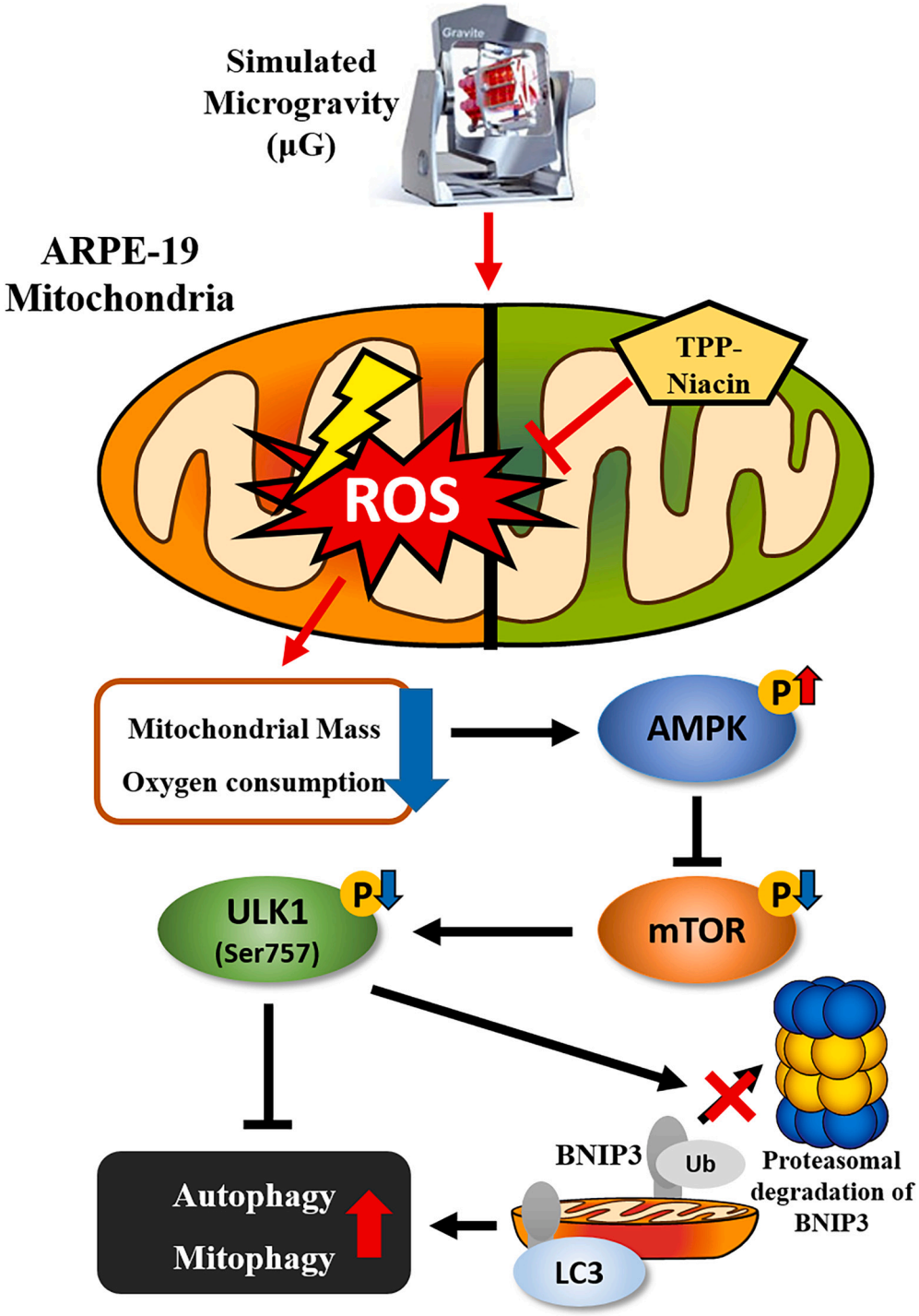

Fig. 5. Graphical summary of microgravity-induced effects on ARPE19 cells.
Microgravity induces oxidative stress, ROS in ARPE19 cells and activates mitophagy *via* AMPK-mTOR-ULK1-BNIP3 signaling pathways. Mitochondrial dysfunction is considerably diminished by TPP-Niacin treatment, along with ROS reduction under μG and reversing the loss of mitochondrial mass, which is linked with BNIP3 protein stability.

extended periods of space travel [4], and microgravity was implicated as one of the reasons for causing visual impairment through oxidative stress on the retina [1,2,4]. Mitochondria in ocular cells exposed to visible light generate ROS *via* photosensitization reactions and as a by-product of cellular respiration [6,8,9]. ROS is implicated in many physiological processes, including mitochondrial dysfunction associated with autophagy [1,6,7,11]. Autophagy is a process that removes aggregated proteins and damaged cellular organelles to maintain the homeostatic function of the cell. Autophagy is also induced in response to oxidative stress caused by ROS [11–14,23].

In the present study, we demonstrated that μG induces MCS and decreases cell migration potency in ARPE19 cells, which agrees with other studies using similar clinostat devices [18–21]. The most optimal studies for understanding the effect of space flight on ARPE19 cells will be done onboard the International Space Station (ISS); nevertheless, studies investigating the impact of microgravity exerted on ARPE19 cells on the earth will also provide valuable physiological data because the effects of microgravity and space radiation can be separately measured

and analyzed.

Next, we showed that μG increases intracellular ROS and causes mitochondrial dysfunction in ARPE19 cells, which are cell types that consume high amounts of energy and cause the most oxidative-damaged on the retina. Oxidative stress-induced ROS accumulation results in dramatic impairment of mitochondrial function, shown by fluorescently quantified mitochondrial mass and the prominent biomarker expression of CypD. A mitochondrial chaperone protein, CyD is regulates coupling of electron chain transfer and ATP synthesis *via* mitochondrial permeability transition pore [24]. In this study, reduced expression of CyD agreed with reduced oxygen consumption and ATP synthesis in ARPE19 cells under μG. We also found that μG causes mitochondrial dysfunction at the transcriptional level, which is demonstrated by dramatic down-regulation of mRNA expression of ATP5F1A, a core component of functional ATP synthase. Consequently, μG-induced oxidative stress results in mitochondrial dysfunction in ARPE19 cells under μG.

The efficacy of TPP-Niacin, a mitochondria-targeted antioxidant, has been demonstrated in our previous study using a hydrogen peroxide-induced oxidative stress model in human retinal pigment epithelium cells. Therefore, we evaluated the efficacy of TPP-Niacin against μG-induced oxidative stress and the resulting mitochondrial dysfunction. As a result, we demonstrated that TPP-Niacin reverted the phenotypes caused by μG; TPP-Niacin protected ARPE19 cells from μG-induced ROS production and mitochondrial mass reduction.

For the possible underlying mechanism associated with μG-induced ROS production and mitochondrial dysfunction, activation of autophagic pathways was investigated, showing upregulation of autophagic genes such as LC3, p62, and Beclin1. In addition, the proteins involved in the initiation of autophagosome formation, such as VPS34, ATG101, and ATG5-ATG12, are elevated under μG conditions.`.

Because ciliogenesis has been recently implicated with nutrient-dependent autophagy, we also explored and confirmed with confocal microscopy that μG induces ciliogenesis.

Finally, we showed that the p-AMPK/AMPK ratio increases while the ratios of p-mTOR/mTOR and p-ULK1/ULK1 at serine 757 decrease under μG. Because ULK1-dependent autophagy is regulated by AMPK and mTOR, and ULK1 promotes BNIP3 protein stability by preventing its degradation, we confirmed that the protein level of BNIP3 is elevated under μG, indicating activation of mitophagy. Consequently, the elevated level of BNIP3 under μG was reversed with TPP-Niacin treatment, implying that μG-induced mitophagy by regulating ROS production in mitochondria.

5. Conclusion

This study shows that μG induces oxidative stress by producing intracellular ROS in ARPE19 cells and activates mitophagy *via* AMPK-mTOR-ULK1-BNIP3 signaling pathways. Mitochondrial dysfunction associated with μG-induced oxidative stress is considerably diminished by TPP-Niacin treatment, along with ROS reduction under μG and reversing the loss of mitochondrial mass, which is linked with BNIP3 protein stability. These results provide the first experimental evidence for TPP-Niacin as a potential therapeutic agent to ameliorate the cellular phenotypes caused by microgravity in ARPE19 cells (Fig. 5. Graphical summary). Further investigations are required to determine its physiological functions and biological efficacies in primary human retinal cells and *in vivo* models and target identification.

CRedit authorship contribution statement

Hong Phuong Nguyen: Investigation, Writing. **Seungheon Shin**: Conceptualization, Visualization, and Writing. **Kyung-Ju Shin**: Conceptualization,Writing - review & editing.

Phuong Hoa Tran: Investigation. **Hyungsun Park**: Investigation. **Quang De Tran**: Investigation. **Mi-Hyun No**: Investigation. **Ji Su Sun**: Investigation. **Ki Woo Kim**: Conceptualization. **Hyo-Bum Kwak**: Conceptualization. **Seongju Lee**: Conceptualization.

Steve K. Cho: Conceptualization, and Writing - review & editing. **Su-Geun Yang**: Conceptualization, Writing - review & editing, and Project administration.

Declaration of competing interest

The authors declare that they have no known competing financial interests or personal relationships that could have appeared to influence the work reported in this paper.

Data availability

Data will be made available on request.

Acknowledgements

This work was supported by the Basic Science Research Program and the Bio & Medical Technology Development Program of the National Research Foundation (NRF) funded by the Korean government (MOE and MSIT) (2020R1A2B5B02002377, 2018R1A6A1A03025523, and 2019M3E5D1A02069623).

References

[1] H.P. Nguyen, et al., The effects of real and simulated microgravity on cellular mitochondrial function, NPJ Microgravity 7 (1) (2021) 44.
[2] F. Cialdai, et al., Effect of space flight on the behavior of human retinal pigment epithelial ARPE-19 cells and evaluation of coenzyme Q10 treatment, Cell. Mol. Life Sci. 78 (23) (2021) 7795–7812.
[3] A.G. Lee, et al., Spaceflight associated neuro-ocular syndrome (SANS) and the neuro-ophthalmologic effects of microgravity: a review and an update, NPJ Microgravity 6 (2020) 7.
[4] E.G. Overbey, et al., Spaceflight influences gene expression, photoreceptor integrity, and oxidative stress-related damage in the murine retina, Sci. Rep. 9 (1) (2019) 13304.
[5] J. Lee, S. Giordano, J. Zhang, Autophagy, mitochondria and oxidative stress: cross-talk and redox signalling, Biochem. J. 441 (2) (2012) 523–540.
[6] M.D. Subramaniam, et al., Oxidative stress and mitochondrial transfer: a new dimension towards ocular diseases, Genes & Diseases 9 (3) (2022) 610–637.
[7] M.H. Kim, et al., Improved effect of a mitochondria-targeted antioxidant on hydrogen peroxide-induced oxidative stress in human retinal pigment epithelium cells, BMC Pharmacol. Toxicol. 22 (1) (2021) 7.
[8] A.X. Chen, et al., Functional imaging of mitochondria in retinal diseases using flavoprotein fluorescence, Eye (Lond) 35 (1) (2021) 74–92.
[9] L. Singh, M.K. Singh, Mitochondria and Eye, Mutagenesis and Mitochondrial-Associated Pathologies (2021) 137–144. IntechOpen.
[10] K.M. Lee, et al., Disruption of the cereblon gene enhances hepatic AMPK activity and prevents high-fat diet-induced obesity and insulin resistance in mice, Diabetes 62 (6) (2013) 1855–1864.
[11] A.J. Jeong, et al., Microgravity induces autophagy via mitochondrial dysfunction in human Hodgkin's lymphoma cells, Sci. Rep. 8 (1) (2018) 14646.
[12] C.W. Park, et al., BNIP3 is degraded by ULK1-dependent autophagy via MTORC1 and AMPK, Autophagy 9 (3) (2013) 345–360.
[13] A. Gao, et al., Bnip3 in mitophagy: novel insights and potential therapeutic target for diseases of secondary mitochondrial dysfunction, Clin. Chim. Acta 506 (2020) 72–83.
[14] G. Battogtokh, et al., Mitochondria-targeting drug conjugates for cytotoxic, anti-oxidizing and sensing purposes: current strategies and future perspectives, Acta Pharm. Sin. B 8 (6) (2018) 862–880.
[15] Y. Zhang, et al., A mitochondria-targeted dual-functional aggregation-induced emission luminogen for intracellular mitochondrial imaging and photodynamic therapy, Biomater Sci 9 (4) (2021) 1232–1236.
[16] B. Ozsvari, F. Sotgia, L. MP, Exploiting mitochondrial targeting signal(s), TPP and bis-TPP, for eradicating cancer stem cells (CSCs). Aging (Albany NY). 10 (2) (2018) 229–240.
[17] J. Zielonka, et al., Mitochondria-targeted triphenylphosphonium-based compounds: syntheses, mechanisms of action, and therapeutic and diagnostic applications, Chem. Rev. 117 (15) (2017) 10043–10120.
[18] T. Furukawa, et al., Simulated microgravity attenuates myogenic differentiation via epigenetic regulations, NPJ Microgravity 4 (2018) 11.
[19] Y.J. Kim, et al., Time-averaged simulated microgravity (taSMG) inhibits proliferation of lymphoma cells, L-540 and HDLM-2, using a 3D clinostat, Biomed. Eng. Online 16 (1) (2017).
[20] C. Buken, et al., Morphological and molecular changes in juvenile Normal human fibroblasts exposed to simulated microgravity, Sci. Rep. 9 (1) (2019) 11882.
[21] D. Grimm, et al., The effects of microgravity on differentiation and cell growth in stem cells and cancer stem cells, Stem Cells Transl. Med. 9 (8) (2020) 882–894.

[22] X.W. Mao, et al., Spaceflight environment induces mitochondrial oxidative damage in ocular tissue, Radiat. Res. 180 (4) (2013) 340–350.
[23] L.P. Poole, et al., ULK1 promotes mitophagy via phosphorylation and stabilization of BNIP3, Sci. Rep. 11 (1) (2021) 20526.
[24] G.A. Porter Jr., G. Beutner, D. Cyclophilin, Somehow a master regulator of mitochondrial function, Biomolecules 8 (4) (2018).
[25] S. Yang, J. Zhou, D. Li, Functions and diseases of the retinal pigment epithelium, Front. Pharmacol. 12 (2021), 727870.